

Received August 7, 2021, accepted September 10, 2021, date of publication September 20, 2021, date of current version October 11, 2021.

Digital Object Identifier 10.1109/ACCESS.2021.3114169

Mixing Matrix Estimation Algorithm for Underdetermined Blind Source Separation

WEIHONG FU¹, XIAOWEI BAI¹, FAN SHI², CHUNHUA ZHOU³, AND YONGYUAN LIU⁴

¹School of Telecommunications Engineering, Xidian University, Xi'an, Shaanxi 710071, China

²Shenzhen GrenTech WL Communication Ltd., Shenzhen 518028, China

³Shanghai Radio Equipment Research Institute, Shanghai 201109, China

⁴Rayfond Technology Company Ltd., Beijing 100094, China

Corresponding author: Weihong Fu (whfu@mail.xidian.edu.cn)

This work was supported by the Natural Science Foundation of Shanghai under Grant 19ZR1454000.

ABSTRACT An original algorithm for underdetermined mixing matrix estimation is proposed in this paper, which can estimate the mixing matrix effectively when the number of source signals is unknown. Firstly, a new single source point (SSP) detection algorithm based on transform matrix is proposed, which can effectively detect single source time-frequency (TF) points by using the characteristics of complex ratio and improve the sparsity of source signals. In view of the fact that the number of source signals is unknown, a novel estimation algorithm based on element sorting is proposed, which can significantly improve the estimation accuracy of the number of source signals. Finally, the mixing matrix is estimated by using the cluster center obtained by agglomerative hierarchical clustering (AHC) algorithm. The simulation results show that the proposed algorithm can improve the estimation accuracy of the number of source signals and underdetermined mixing matrix obviously, and the algorithm has higher robustness compared with other algorithms.

INDEX TERMS Underdetermined blind source separation, mixing matrix estimation, single-source point detection, agglomerative hierarchical clustering.

I. INTRODUCTION

Blind source separation (BSS) refers to the process of separating and recovering signals by using only the observed signals when the source signals and the transmission channel are unknown [1]. After years of research and development, BSS has been successfully applied in many fields, including military communications [2], image processing [3], speech signal processing [4], and other fields. BSS is defined as underdetermined blind source separation (UBSS) when the number of observed signals is less than the number of source signals [5]. Due to the particularity of underdetermined mixing model, many algorithms for overdetermined and normal determined models are not suitable for UBSS [6]. At present, two-step method is the main method to solve UBSS problem. The first step is to estimate the mixing matrix, and the second step is to recover the source signals according to the obtained mixing matrix [7]. There is no doubt that the estimation accuracy of mixing matrix directly affects the recovery results of source signals. Underdetermined mixing matrix estimation

mainly depends on the sparsity of the source signals [8]. Sparse component analysis (SCA) can effectively estimate the underdetermined mixing matrix [9]. If the source signals are sufficiently sparse in time domain, the observed signals can be processed directly. For example, in [10], it is assumed that the source signals are sparse in time domain. The ratios of the observed signals are calculated firstly, and the number of the source signals and the mixing matrix are determined by using the large number theorem and the bar graph. Fu [11] proposed a mixing matrix estimation algorithm based on similarity measurement. The ranking matrix is constructed and the underdetermined mixing matrix is estimated by clustering analysis. However, when the sparsity of the source signals in the time domain is poor, these algorithms are no longer applicable. Nong and Fu [12] proposed an underdetermined mixing matrix estimation algorithm based on homogeneous polynomials. By using algebraic geometry theory, the mixing matrix can be estimated without the influence of convergence. In fact, the short-time Fourier transform (STFT) is usually used to transform the observed signals from the time domain to the corresponding TF domain [13]. The sparsity of signals can be effectively improved by using SSPs in TF domain.

The associate editor coordinating the review of this manuscript and approving it for publication was Wei Wang¹.

In [14], Kmeans clustering algorithm is used to estimate the mixing matrix, but the algorithm needs to know the number of clusters and is sensitive to noise and the initial cluster center. An SSP detection algorithm is proposed in [15], which can effectively estimate the mixing matrix by using SSPs, but large computational complexity is the main defects. Ye *et al.* [16] proposed an SSP detection algorithm based on the transformation matrix, and then determined the number of source signals by looking for the peak value of the potential function, but the selection of peak value is greatly affected by the noise. The algorithms in [17]–[21] all use SSP detection to improve the sparsity of the source signals. Then the mixing matrix is estimated by clustering analysis. However, there are still some problems in the existing algorithms, such as too much computation or poor robustness. For the determination of the number of source signals, it is usually assumed to be known, but it does not meet the actual requirements. The existing estimation algorithms have low accuracy or poor stability. When the estimation of the number of source signals is wrong, the wrong mixing matrix is often obtained. Therefore, the underdetermined mixing matrix estimation is still worthy of further study.

In this paper, we propose a mixing matrix estimation algorithm for UBSS. First, a new SSP detection algorithm based on transform matrix is proposed to improve the sparsity of signals. Next, a novel estimation algorithm based on element ordering is proposed to determine the number of source signals. Lastly, the mixing matrix is estimated by using the AHC algorithm.

The rest of this paper is organized as follows. Section 2 introduces the basic models of UBSS, and Section 3 describes the underdetermined mixing matrix estimation algorithm, including SSP detection algorithm, estimation algorithm of the number of source signals, and AHC algorithm. Section 4 shows the simulation results and analysis, and the conclusions are drawn in Sec. 5.

II. BASIC MODELS

The linear instantaneous mixing model of the UBSS problem can be denoted as

$$x(t) = As(t) + n(t). \quad (1)$$

where $x(t) = [x_1(t), x_2(t), \dots, x_M(t)]^T$ is the observed signals vector; $A = [a_1, a_2, \dots, a_N] \in \mathbb{C}^{M \times N}$ ($M < N$) is the mixing matrix; $a_n (n = 1, 2, \dots, N)$ is the column vector of mixing matrix; $s(t) = [s_1(t), s_2(t), \dots, s_N(t)]^T$ is the source signals vector; M and N are the numbers of observed signals and source signals, respectively. $n(t)$ is the additive white Gaussian noise.

If the source signals are from the far field and meet the narrow-band condition, the mixing matrix can be written as (2), as shown at the bottom of the next page, where $f_n (n = 1, 2, \dots, N)$ is the frequency of source signal s_n , d is the distance between two adjacent receiving sensors, $\theta_n \in (-\pi/2, \pi/2)$ is the direction of arrival (DOA) of s_n ,

and c is the light speed. Here, we set $d = \lambda_{\min}/2$, where λ_{\min} is the minimum wavelength of source signal.

Equation (2) can be simplified as

$$A = \begin{bmatrix} 1 & 1 & \dots & 1 \\ e^{j\gamma_1} & e^{j\gamma_2} & \dots & e^{j\gamma_N} \\ \vdots & \vdots & \dots & \vdots \\ e^{j(M-1)\gamma_1} & e^{j(M-1)\gamma_2} & \dots & e^{j(M-1)\gamma_N} \end{bmatrix} \quad (3)$$

where $\gamma_n = 2\pi f_n d \sin \theta_n / c$ ($n = 1, 2, \dots, N$). Without the influence of noise, we can obtain (4) from (1) and (3).

$$\begin{bmatrix} x_1(t) \\ x_2(t) \\ \vdots \\ x_M(t) \end{bmatrix} = \begin{bmatrix} 1 & 1 & \dots & 1 \\ e^{j\gamma_1} & e^{j\gamma_2} & \dots & e^{j\gamma_N} \\ \vdots & \vdots & \dots & \vdots \\ e^{j(M-1)\gamma_1} & e^{j(M-1)\gamma_2} & \dots & e^{j(M-1)\gamma_N} \end{bmatrix} \cdot \begin{bmatrix} s_1(t) \\ s_2(t) \\ \vdots \\ s_N(t) \end{bmatrix} \quad (4)$$

III. MIXING MATRIX ESTIMATION FOR UBSS

A. SSP DETECTION

Underdetermined mixing matrix estimation requires the signals to be sparse, but in practice, the source signals often have poor sparsity in the time domain. Therefore, we first use STFT to transform the observed signals into the TF domain. For simplicity, take two observed signals as an example ($M = 2$), and (4) can be expressed as

$$\begin{bmatrix} X_1(t, f) \\ X_2(t, f) \end{bmatrix} = \begin{bmatrix} 1 & 1 & \dots & 1 \\ e^{j\gamma_1} & e^{j\gamma_2} & \dots & e^{j\gamma_N} \end{bmatrix} \begin{bmatrix} S_1(t, f) \\ S_2(t, f) \\ \vdots \\ S_N(t, f) \end{bmatrix} = \begin{bmatrix} S_1(t, f) + S_2(t, f) + \dots + S_N(t, f) \\ S_1(t, f)e^{j\gamma_1} + S_2(t, f)e^{j\gamma_2} + \dots + S_N(t, f)e^{j\gamma_N} \end{bmatrix} \quad (5)$$

where $X_m(t, f) (m = 1, 2)$ and $S_n(t, f) (n = 1, 2, \dots, N)$ are the STFT coefficients of the observed signals and the source signals respectively. When only one source signal $s_n (n = 1, 2, \dots, N)$ exists at a TF domain point, the ratio of the observed signals in the TF domain (we simply refer to the ratio of the observed signals in the following) can be obtained

$$\frac{X_2(t, f)_n}{X_1(t, f)_n} = e^{j\gamma_n}, \quad (n = 1, 2, \dots, N) \quad (6)$$

where $e^{j\gamma_n} (n = 1, 2, \dots, N)$ is the theoretical ratio determined by s_n , $\gamma_n (n = 1, 2, \dots, N)$ is the theoretical ratio phase angle. It can be seen from (6) that the ratio of $X_2(t, f)_n / X_1(t, f)_n$ actually calculated is a complex number. The traditional clustering algorithm is no longer suitable in the complex field, hence the transformation matrix \mathbf{T} is introduced to solve the clustering problem of complex

numbers [16].

$$\mathbf{T} = \begin{bmatrix} 1 & 1 \\ e^{j\frac{\pi}{2}} & e^{-j\frac{\pi}{2}} \end{bmatrix} \quad (7)$$

According to (5) and (7), we can obtain

$$\begin{aligned} & \begin{bmatrix} X'_1(t, f) \\ X'_2(t, f) \end{bmatrix} \\ &= \mathbf{T} \begin{bmatrix} X_1(t, f) \\ X_2(t, f) \end{bmatrix} \\ &= \begin{bmatrix} 1 & 1 \\ e^{j\frac{\pi}{2}} & e^{-j\frac{\pi}{2}} \end{bmatrix} \begin{bmatrix} X_1(t, f) \\ X_2(t, f) \end{bmatrix} \\ &= \begin{bmatrix} 1 & 1 \\ e^{j\frac{\pi}{2}} & e^{-j\frac{\pi}{2}} \end{bmatrix} \begin{bmatrix} 1 & 1 & \dots & 1 \\ e^{j\gamma_1} & e^{j\gamma_2} & \dots & e^{j\gamma_N} \end{bmatrix} \\ & \quad \times \begin{bmatrix} S_1(t, f) \\ S_2(t, f) \\ \vdots \\ S_N(t, f) \end{bmatrix} \\ &= \begin{bmatrix} S_1(t, f) + S_2(t, f) + \dots + S_N(t, f) + \\ e^{j\gamma_1} S_1(t, f) + e^{j\gamma_2} S_2(t, f) + \dots + e^{j\gamma_N} S_N(t, f) \\ e^{j\frac{\pi}{2}} (S_1(t, f) + S_2(t, f) + \dots + S_N(t, f)) + e^{-j\frac{\pi}{2}} \\ (e^{j\gamma_1} S_1(t, f) + e^{j\gamma_2} S_2(t, f) + \dots + e^{j\gamma_N} S_N(t, f)) \end{bmatrix} \end{aligned} \quad (8)$$

where $\mathbf{X}'(t, f) = [X'_1(t, f) X'_2(t, f)]^T$ is the observed signals vector reconstructed after introducing the transformation matrix \mathbf{T} . When only one source signal s_n ($n = 1, 2, \dots, N$) exists in a TF domain point, we can obtain

$$\begin{aligned} \frac{X'_2(t, f)_n}{X'_1(t, f)_n} &= \frac{e^{j\frac{\pi}{2}} + e^{j(-\frac{\pi}{2} + \gamma_n)}}{e^{j\gamma} + e^{j(0 + \gamma_n)}} \\ &= \frac{[e^{j\frac{\pi}{2}} + e^{j(-\frac{\pi}{2} + \gamma_n)}] e^{-j\frac{\gamma_n}{2}} e^{j\frac{\gamma_n}{2}}}{[e^{j0} + e^{j(\gamma_n)}] e^{-j\frac{\gamma_n}{2}} e^{j\frac{\gamma_n}{2}}} \\ &= \frac{[e^{j(\pi - \gamma_n)/2} + e^{-j(\pi - \gamma_n)/2}] e^{j\frac{\gamma_n}{2}}}{[e^{j(-\gamma_n)/2} + e^{-j(-\gamma_n)/2}] e^{j\frac{\gamma_n}{2}}} \\ &= \frac{\cos[(\pi - \gamma_n)/2]}{\cos[(-\gamma_n)/2]} \\ &= \frac{\sin[(\gamma_n)/2]}{\cos[(-\gamma_n)/2]} = \tan\left(\frac{\gamma_n}{2}\right) \end{aligned} \quad (9)$$

where $X'_1(t, f)_n$ and $X'_2(t, f)_n$ are both complex numbers. When the ratio of the two complex numbers is a real constant,

the following formula can be obtained.

$$\frac{\text{Im}(X'_2(t, f)_n)}{\text{Re}(X'_2(t, f)_n)} = \frac{\text{Im}(X'_1(t, f)_n)}{\text{Re}(X'_1(t, f)_n)} \quad (10)$$

where $\text{Re}(\cdot)$ and $\text{Im}(\cdot)$ denote the real and imaginary parts of data, respectively.

However, in practice, the results obtained are not in accordance with the above formula under the influence of noise and calculation error. Therefore, we reduce the detection standard and use the following formula to detect SSP.

$$\left| \frac{\text{Im}(X'_2(t, f)_n)}{\text{Re}(X'_2(t, f)_n)} - \frac{\text{Im}(X'_1(t, f)_n)}{\text{Re}(X'_1(t, f)_n)} \right| < \varepsilon_1 \quad (11)$$

where ε_1 is a positive number approximate to 0, and the TF point (t, f) satisfying Eq. (11) is the SSP TF point. In this paper, we set $\varepsilon_1 = 0.02$. The number of all SSPs of observed signals is assumed to be I , and $X'_2(t_i, f_i)/X'_1(t_i, f_i)$ ($i = 1, 2, \dots, I$) is the corresponding ratio of the two observed signals in the TF domain after introducing transformation matrix T . $X'_2(t_i, f_i)/X'_1(t_i, f_i)$ is generally a complex number rather than a real number due to the influences of computer precision and calculation error, and the clustering algorithm still cannot be used directly. Therefore, $\hat{\gamma}_i$ ($i = 1, 2, \dots, I$) is calculated first, and its definition is as follows

$$\hat{\gamma}_i \triangleq 2 \tan^{-1} \left(\frac{\text{Re}(X'_2(t_i, f_i))}{\text{Re}(X'_1(t_i, f_i))} \right) \quad (12)$$

It is important to note that after SSP detection, a large number of low energy points will still gather near the origin, which will reduce the estimation accuracy and improve the complexity. Therefore, we use (13) to eliminate low energy points.

$$\left(\frac{\|X'(t, f)\|_2}{\max(\|X'(t, f)\|_2)} \right) < \varepsilon_2 \quad (13)$$

where $X'(t, f) = [X'_1(t, f) X'_2(t, f)]^T$, and ε_2 is a positive number approximate to 0. $\|\cdot\|_2$ represents the computation of vector norms. The TF point satisfying (13) is a low-energy point and an appropriate value of ε_2 should be selected. Here, we set $\varepsilon_2 = 0.5$.

The number of TF points after the SSP detection and elimination of low-energy points is assumed to be P , and (t_p, f_p) ($p = 1, 2, \dots, P$) is the corresponding TF point.

$$\mathbf{A} = \begin{bmatrix} 1 & 1 & \dots & 1 \\ e^{j\frac{2\pi f_1 d \sin \theta_1}{c}} & e^{j\frac{2\pi f_2 d \sin \theta_2}{c}} & \dots & e^{j\frac{2\pi f_N d \sin \theta_N}{c}} \\ \vdots & \vdots & \vdots & \vdots \\ e^{j\frac{2\pi f_1 (M-1)d \sin \theta_1}{c}} & e^{j\frac{2\pi f_2 (M-1)d \sin \theta_2}{c}} & \dots & e^{j\frac{2\pi f_N (M-1)d \sin \theta_N}{c}} \end{bmatrix} \quad (2)$$

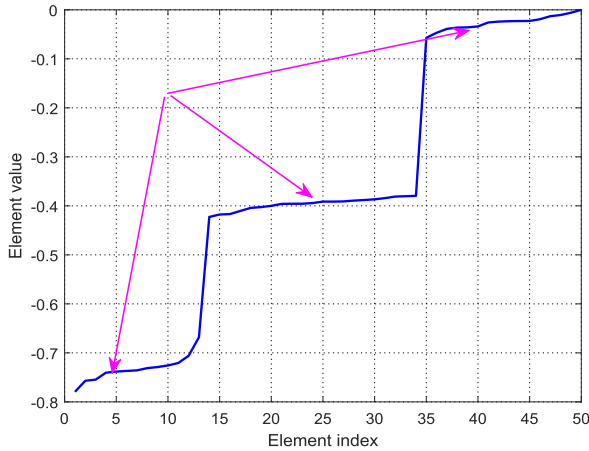


FIGURE 1. Values of the k th ($k = 1, 2, \dots, P$) column vector of matrix $D_{P \times P}$.

According to (12), we can define

$$\hat{\gamma}_p \triangleq 2 \tan^{-1} \left(\frac{X'_2(t_p, f_p)}{X'_1(t_p, f_p)} \right) \quad (p = 1, 2, \dots, P) \quad (14)$$

Finally, the AHC algorithm is adopted to obtain the cluster centers by using $\hat{\gamma}_p$ ($p = 1, 2, \dots, P$).

B. ESTIMATION OF THE NUMBER OF SOURCE SIGNALS

The premise of using the AHC clustering algorithm is that the number of source signals is known. Here, we propose a new estimation algorithm based on element sorting for the number of sources.

We first define the distance distribution matrix $D_{P \times P}$ as follows

$$D_{P \times P} = \{d(\hat{\gamma}_{p_1}, \hat{\gamma}_{p_2}) | 1 \leq p_1 \leq P, 1 \leq p_2 \leq P\} \quad (15)$$

where $d(\hat{\gamma}_{p_1}, \hat{\gamma}_{p_2})$ is the distance between $\hat{\gamma}_{p_1}$ and $\hat{\gamma}_{p_2}$.

The row vectors of the matrix $D_{P \times P}$ are arranged in ascending order, and then the column vectors are also arranged in ascending order. The new distance distribution matrix $D'_{P \times P}$ can be obtained after sorting. Here we take $N = 3$ as an example to illustrate the principle of the algorithm. When $N = 3$, the following Fig. 1 can be obtained by using the k th ($k = 1, 2, \dots, P$) column vector of matrix $D'_{P \times P}$.

As shown in the Fig. 1, the number of source signals corresponding to the line segments with a slope of approximately 0 indicated by the arrows. Then we use the following rule to determine the number of source signals.

The difference results of the k th column vector are shown in Fig. 2.

$$D_{\{k\}(p+1)} - D_{\{k\}(p)} > \beta \quad (1 \leq p \leq P - 1) \quad (16)$$

As shown in the Fig. 2, the number of source signals should be the number of peaks plus 1. Therefore, we can introduce appropriate parameter β to determine the number of peaks and then determine the number of source signals. Here, we set $\beta = 0.15$.

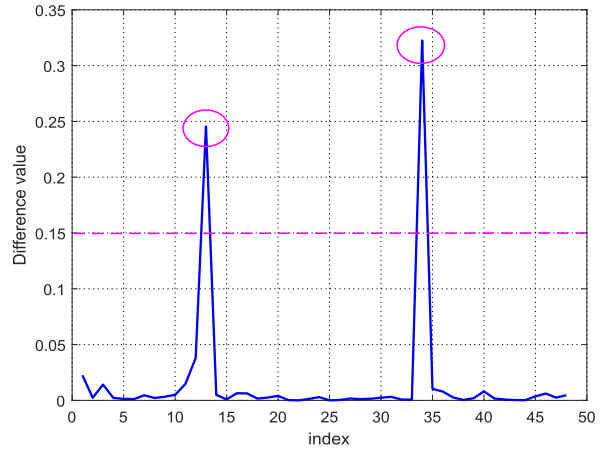


FIGURE 2. Difference values of the k th ($k = 1, 2, \dots, P$) column vector of matrix $D_{P \times P}$.

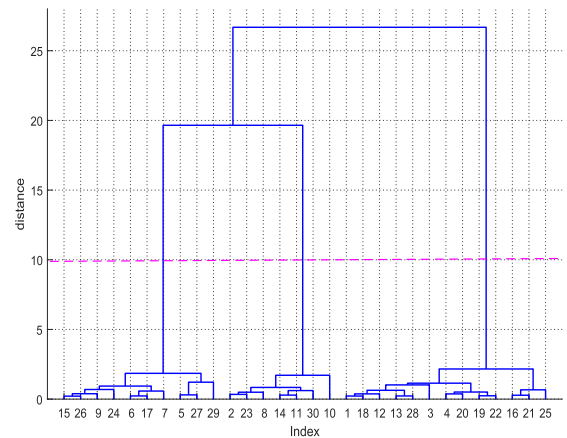


FIGURE 3. Difference values of the k th ($k = 1, 2, \dots, P$) column vector of matrix $D'_{P \times P}$.

C. AHC ALGORITHM

Agglomerative hierarchical clustering is a hierarchical clustering algorithm with bottom-up aggregation strategy. First, each sample in the dataset is regarded as an initial cluster, and then the nearest two clusters are found for merging at each step of the algorithm. The process is repeated until the number of clusters reaches the preset number and we can get a hierarchical clustering tree, as shown in the Fig.3.

As shown by the dotted line in the Fig. 3, after determining the number of source signals, we can get the corresponding different clusters. In the process of clustering, there are three main ways to measure the distance between classes, as shown in (17).

$$\begin{cases} d_{\min}(C_i, C_j) = \min_{k \in C_i, q \in C_j} \text{dist}(k, q) \\ d_{\max}(C_i, C_j) = \max_{k \in C_i, g \in C_j} \text{dist}(k, q) \\ d_{\text{ang}}(C_i, C_j) = \frac{1}{|C_i| |C_j|} \sum_{k \in C_i} \sum_{q \in C_j} \text{dist}(k, q) \end{cases} \quad (17)$$

In this paper, we use $d_{avg}(C_i, C_j)$ to calculate the distance between clusters. Finally, the average value of each cluster is calculated as the cluster center and the mixing matrix can be estimated as

$$\hat{A} = \begin{bmatrix} 1 & 1 & \dots & 1 \\ e^{jc_1} & e^{jc_2} & \dots & e^{jc_N} \end{bmatrix} \quad (18)$$

The main steps of the AHC clustering are as follows:

Input : $\hat{\gamma}_p (p = 1, 2, \dots, P)$
 Output : $c_i (i = 1, 2, \dots, N)$

step:

1. Each $\hat{\gamma}_p$ is an initial cluster;
2. Repeat:
 - 2.1 Calculate the distance between any two clusters, and find the nearest two clusters;
 - 2.2 Merge two clusters to generate a new cluster;
3. Until: Reaches the given number of clusters;
4. Calculate the mean value of each cluster.

In summary, the steps of underdetermined mixing matrix estimation algorithm for UBSS are as follows

- (1) STFT is used to transform the observed signals from the time domain to the TF domain.
- (2) The reconstructed observed signals vector in the TF domain $X'(t, f) = [X'_1(t, f) X'_2(t, f)]^T$ are obtained by using (8) in Sect. 3.1 after introducing transformation matrix T .
- (3) The single-source TF points are detected using (11) in Sect. 3.1.
- (4) The low-energy points are eliminated using (13), and $\hat{\gamma}_p (p = 1, 2, \dots, 2P)$ is obtained by using (14) in Sect. 3.1.
- (5) The number of source signals is estimated using the estimation algorithm based on the element sorting in Sect. 3.2.
- (6) The AHC algorithm is used to obtain the cluster centers, and the mixing matrix is estimated using (18) in Sect. 3.3.

IV. SIMULATION AND RESULT ANALYSIS

In this paper, three groups of experiments are conducted to prove the performance of the proposed algorithm. Experiment 1 shows the results of the SSP detection and low energy points elimination. Experiment 2 shows performance of the source number estimation algorithm based on element sorting. Experiment 3 shows the comparison between the proposed algorithm and other algorithm for mixing matrix estimation of UBSS. The noise in the experiment is white Gaussian noise. The normalized mean square error (NMSE) of the mixing matrix is adopted in the experiments to measure the estimation accuracy. It is defined as

The normalized mean square error (NMSE) of the mixing matrix is adopted in the experiments to measure the estimation accuracy. It is defined as

$$NMSE = 10 \log \left(\frac{\sum_{i,j} (\hat{a}_{i,j} - a_{i,j})^2}{\sum_{i,j} a_{i,j}^2} \right) \quad (19)$$

TABLE 1. Radar signals parameters.

s_i	Signal type	f_i (MHz)	bandwidth(MHz)	DOA(rad)
s_1	Conventional pulse radar signal	60	/	0.39
s_2	Conventional pulse radar signal	70	/	1.31
s_3	linear frequency modulated radar signal	200	6	0.22
s_4	linear frequency modulated radar signal	150	6	0.77
s_5	linear frequency modulated radar signal	120	6	1.50

TABLE 2. Simulation parameters of the proposed algorithm.

Sampling frequency	STFT size	Overlapping	Window length	Window function	ϵ_1	ϵ_2	β
500MHz	1024	256	1024	Hann	0.02	0.5	0.15

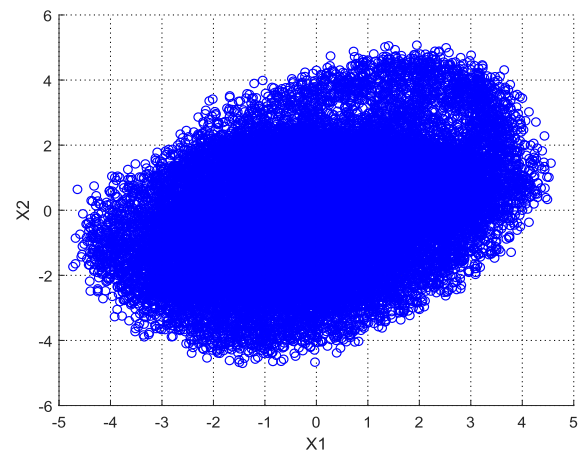


FIGURE 4. Scatter plot of received signals after STFT.

where $a_{i,j}$ is the (i, j) th element of A , and $\hat{a}_{i,j}$ is the (i, j) th element of \hat{A} . A is the actual mixing matrix, and \hat{A} is the estimated mixing matrix.

Five radar source signals are given in the experiment and the parameters are shown in Table. 1.

The simulation parameters of the proposed algorithm are shown in Table. 2.

A. SIMULATION OF THE PROPOSED SSP DETECTION ALGORITHM

Fig. 4 is the scatter plot of observed signals after STFT when Signal-to-Noise (SNR) is 15dB.

As shown in the Fig. 4, after STFT, the line characteristics of the TF point coefficients are not obvious. Therefore, these TF points cannot be directly used for mixing matrix estimation. Fig. 5 is the scatter plot of observed signals after SSP detection. As shown in the Fig. 5, after SSP detection, the reconstructed observed signals have obvious linear characteristics. The scatter points in the Fig. 5 are clustered on five straight lines with different slopes, which exactly correspond to the number of source signals. However, there are still a large number of low energy points near the origin. These low

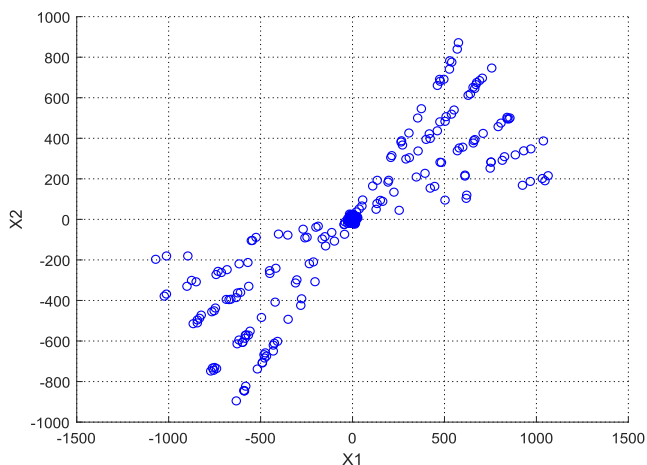


FIGURE 5. Scatter plot after SSP detection.

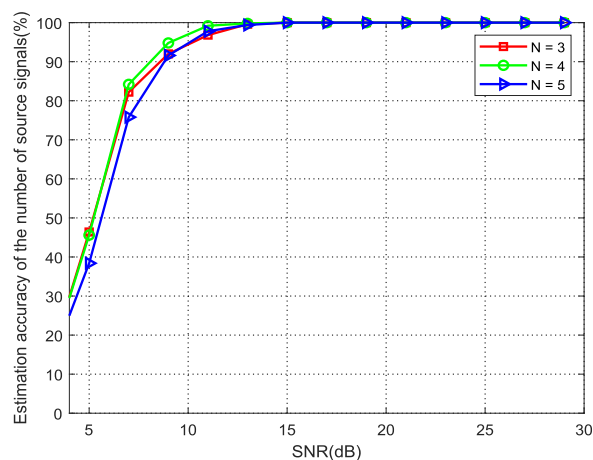


FIGURE 7. Estimation accuracy of the proposed algorithm under different numbers of source signals.

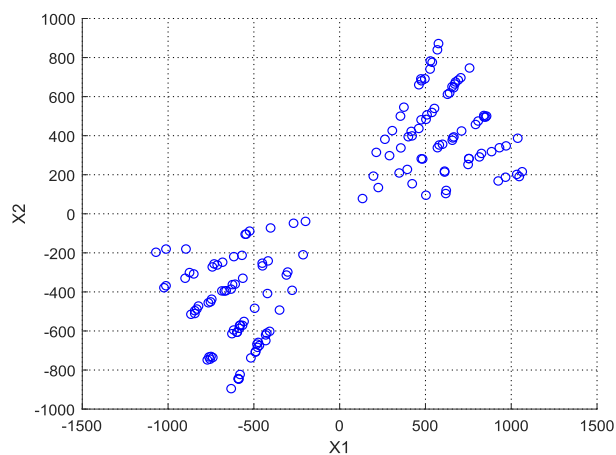


FIGURE 6. Scatter plot after SSP detection and eliminating low energy points.

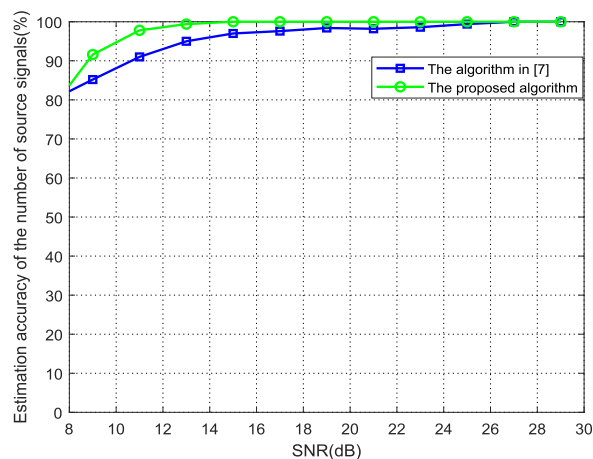


FIGURE 8. Clustering correction rate of the different clustering algorithm under different number of source signals.

energy points will affect the estimation of mixing matrix, so it is necessary to eliminate these low energy SSPs.

Fig. 6 is the scatter plot of observed signals after SSP detection and eliminating low energy points. After eliminating the low energy points, we can make full use of the linear characteristics of the observed signals to estimate the mixing matrix.

B. SIMULATION OF THE PROPOSED ESTIMATION ALGORITHM OF THE NUMBER OF SOURCE SIGNALS BASED ON ELEMENT SORTING

The experiment is performed 100 times under different SNRs from 5 dB to 30 dB when the number of source signals is 3, 4 and 5. The estimation accuracy is the number of times to get the correct number of source signals divided by the total number of simulations. The simulation results are shown in Fig. 7.

Fig. 7 shows the estimation accuracy of the proposed algorithm in three cases within the SNR range of 5–30dB. It can be seen from the Fig. 7 that the estimation results in the three cases are relatively close. The estimation accuracy increases

with the increase of SNR. When SNR is more than 10 dB, the estimation accuracy is more than 90 %. Fig. 8 shows the simulation results of the proposed algorithm and the algorithm in [1] under different SNR when the number of source signals is 5.

Fig. 9 demonstrates that the clustering accuracy in the six different cases. Compared with the other two clustering algorithms, AHC always has higher clustering accuracy in the whole SNR range. Under the same number of sampling points, the less the number of real clusters is, the higher the clustering accuracy can be obtained.

Assuming that the number of source signals has been obtained by the estimation algorithm, Fig. 10 shows the NMSE by using the proposed mixing matrix estimation algorithm under different number of source signals.

The results show that the NMSE values of the mixing matrix are close to each other under three different cases, and the NMSE values are less than -40 dB when the SNR is greater than 10dB. The performance of the proposed algorithm is relatively stable, and it is hardly affected by the number of source signals.

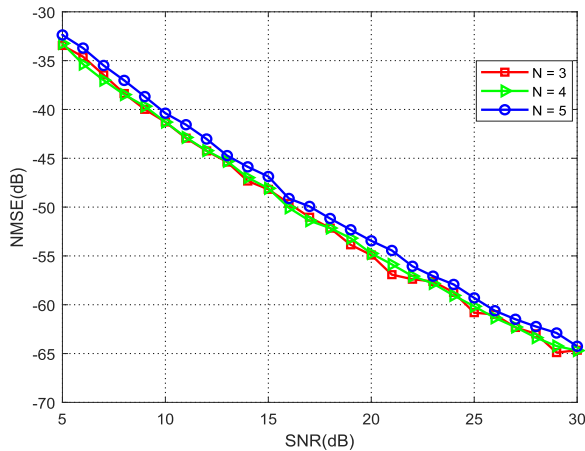


FIGURE 9. Performance of the proposed algorithm with different numbers of source signals.

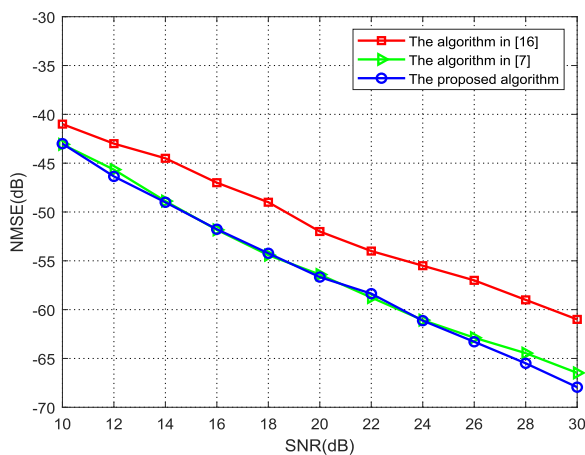


FIGURE 10. Performance of the proposed algorithm with different numbers of source signals.

In order to prove the superiority of the proposed algorithm, this paper compares the proposed algorithm with the algorithm in [7] and [16]. Fig. 10 shows the performance of different algorithms for UBSS under different SNRs. It can be seen from Fig. 10 that the NMSE values of the algorithm proposed in this paper are lower and the performance is better than that of the algorithm in [16]. The higher the SNR is, the lower the NMSE value of the mixing matrix can be obtained. The performance of the proposed algorithm is close to that in [7], but the algorithm in [7] is greatly affected by the initial clustering center, as shown in the Fig. 9. When the initial cluster center is not selected properly, the performance of the algorithm will be greatly affected, and the robustness of the algorithm is poor. The algorithm proposed in this paper can effectively avoid the influence of initial clustering centers, and has better stability under the premise of ensuring accuracy.

V. CONCLUSION

In this paper, a new underdetermined mixing matrix estimation algorithm is proposed. A new single source detection algorithm based on transform matrix is proposed, which can

effectively improve the sparsity of the source signal. We propose a new estimation algorithm based on element ordering, which can improve the estimation accuracy of the number of source signals. Finally, AHC algorithm is used to get the mixing matrix and the mixing matrix estimation error is smaller than the algorithm in reference. The advantages and stability of the proposed algorithm are proved by a number of comparative experiments.

ACKNOWLEDGMENT

The authors would like to thank the anonymous reviewers who read the drafts and provided many helpful suggestions.

REFERENCES

- [1] B. Ma and T. Zhang, "Underdetermined blind source separation based on source number estimation and improved sparse component analysis," *Circuits Syst. Signal Process.*, vol. 5, pp. 1–20, Jan. 2021.
- [2] X. Wang, G. Huang, Z. Zhou, W. Tian, J. Yao, and J. Gao, "Radar emitter intrapulse signal blind sorting under modified wavelet denoising," *J. Eng.*, vol. 2019, no. 21, pp. 8013–8017, Sep. 2019.
- [3] P. Chen, Y. Han, and Y. Li, "X-ray multispectrum CT imaging by projection sequences blind separation based on basis-effect decomposition," *IEEE Trans. Instrum. Meas.*, vol. 70, pp. 1–8, 2021.
- [4] H. D. Do, S. T. Tran, and D. T. Chau, "Speech source separation using variational autoencoder and bandpass filter," *IEEE Access*, vol. 8, pp. 156219–156231, 2020.
- [5] T. Dong, Y. Lei, and J. Yang, "Blind estimation of underdetermined mixing matrix based on density measurement," *Wireless Pers. Commun.*, vol. 104, pp. 26–33, Mar. 2013.
- [6] W. Fu, X. Zhou, and B. Nong, "Oxygen absorption in the earth's atmosphere," *Neurocomputing*, vol. 104, pp. 1283–1300, Nov. 2019.
- [7] X. Bai, W. Fu, and C. Zhou, "Mixing matrix estimation algorithm for time-varying radar signals in a dynamic system under UBSS model," *Circuits Syst. Signal Process.*, vol. 4, pp. 1–24, Jan. 2021.
- [8] Y. Li, W. Nie, F. Ye, and Y. Lin, "A mixing matrix estimation algorithm for underdetermined blind source separation," *Circuits, Syst., Signal Process.*, vol. 35, no. 9, pp. 3367–3379, Nov. 2015.
- [9] H. Liu, L. Zou, J. Wu, L. Zhang, and T. Zhao, "Underdetermined blind source separation algorithm of 220kV substation noise based on SCA," in *Proc. IEEE Int. Conf. High Voltage Eng. Appl. (ICHVE)*, Chengdu, China, Sep. 2016, pp. 1–4.
- [10] P. Xu, Y. Jia, Z. Wang, and M. Jiang, "Underdetermined blind source separation for sparse signals based on the law of large numbers and minimum intersection angle rule," *Circuits, Syst., Signal Process.*, vol. 39, no. 5, pp. 2442–2458, Sep. 2019.
- [11] W. Fu, X. Zhou, and B. Nong, "Blind estimation of underdetermined mixed matrix based on similarity detection," *J. Beijing Univ. Posts Telecommun.*, vol. 40, pp. 24–29, Nov. 2017.
- [12] B. Nong and W. Fu, "Mixing matrix estimation in UBSS based on homogeneous polynomials," *IET Signal Process.*, vol. 12, no. 9, pp. 1123–1130, Dec. 2018.
- [13] Y. Li, X. Geng, X. Guo, Q. Sun, F. Ye, and T. Jiang, "Mixing matrix estimation of frequency hopping signals based on single source points detection," in *Proc. Radio Sci. Meeting (USNC-URSI)*, Atlanta, GA, USA, Jul. 2019, pp. 13–14.
- [14] Y. Xie, K. Xie, Z. Wu, and S. Xie, "Underdetermined blind source separation of speech mixtures based on K-means clustering," in *Proc. Chin. Control Conf. (CCC)*, Guangzhou, China, Jul. 2019, pp. 42–46.
- [15] Y. Chen, Y. Li, and J. Zhou, "Mixing matrix estimation in underdetermined blind source separation based on single source points detection," in *Proc. IEEE 18th Int. Conf. Commun. Technol. (ICCT)*, Chongqing, China, Oct. 2018, pp. 1077–1081.
- [16] F. Ye, J. Chen, L. Gao, W. Nie, and Q. Sun, "A mixing matrix estimation algorithm for the time-delayed mixing model of the underdetermined blind source separation problem," *Circuits, Syst., Signal Process.*, vol. 38, no. 4, pp. 1889–1906, Aug. 2018.
- [17] Q. Guo, G. Ruan, and P. Nan, "Underdetermined mixing matrix estimation algorithm based on single source points," *Circuits, Syst., Signal Process.*, vol. 36, no. 11, pp. 4453–4467, Feb. 2017.

- [18] S. Qin, J. Guo, and C. Zhu, "Sparse component analysis using time-frequency representations for operational modal analysis," *Sensors*, vol. 15, no. 3, pp. 6497–6519, Mar. 2015.
- [19] J. Sun, Y. Li, J. Wen, and S. Yan, "Novel mixing matrix estimation approach in underdetermined blind source separation," *Neurocomputing*, vol. 173, pp. 623–632, Jan. 2016.
- [20] L. Zhang, Z. Ye, Y. Zhang, S. Li, J. Li, and W. Jiang, "Underdetermined mixing matrix estimation based on single source detection," in *Proc. China Int. SAR Symp. (CISS)*, Shanghai, China, Oct. 2018, pp. 1–4.
- [21] L. Zhang, J. Yang, Z. Guo, and Y. Zhou, "Underdetermined blind source separation from time-delayed mixtures based on prior information exploitation," *J. Electr. Eng. Technol.*, vol. 10, no. 5, pp. 2179–2188, Sep. 2015.



WEIHONG FU was born in 1979. She received the M.S. and Ph.D. degrees from Xidian University, Xi'an, Shaanxi, China, in 2004 and 2007, respectively. She is currently an Associate Professor with the School of Communication Engineering, Xidian University. Her current research interests include broadband wireless communication, communication signal processing, and MIMO signal processing.



XIAOWEI BAI received the B.S. degree from Southwest Minzu University, in 2018. He is currently pursuing the M.S. degree with the School of Communication Engineering, Xidian University, Xi'an, Shaanxi, China. His research interests include blind signal processing and communication signal processing.



FAN SHI was born in 1977. He received the M.S. degree from Xidian University, Xi'an, Shaanxi, China, in 2005. He is currently the Technical Director of Shenzhen GrenTech WL Communication Ltd. His current research interests include broadband wireless communication, communication signal processing, and 5G communication.



CHUNHUA ZHOU received the M.S. degree from Northwestern Polytechnical University, in 2004. She is currently a Senior Engineer with Shanghai Radio Equipment Research Institute. Her current research interest includes multi-modal radar cognition of moving targets.



YONGYUAN LIU received the M.S. degree from Xidian University, in 2005. He is currently a Chief Technology Officer at Rayfond Technology Company Ltd., Beijing. His current research interests include wireless communication, emergency communication, and emergency rescue.

...